International Forum on Aeroelasticity and Structural Dynamics
IFASD 2019
9-13 June 2019, Savannah, Georgia, USA

HYSTERETIC RESPONSE OF A LAMINAR AIRFOIL UNDERGOING SINGLE DEGREE OF FREEDOM LIMIT CYCLE OSCILLATIONS IN TRANSONIC FLOW

Marc Braune[1] **and Anne Hebler**[1]

[1] DLR - German Aerospace Center
Institute of Aeroelasticity
Bunsenstraße 10, 37073 Göttingen, Germany
Marc.Braune@dlr.de

Keywords: Laminar Airfoil, Limit Cycle Oscillation, Transonic Flow, Hysteresis, Subcritical Bifurcation, Nonlinear System Response

Abstract: Results of an experimental bifurcation analysis, obtained during a 2D flutter experiment in transonic flow on a CAST 10-2 supercritical laminar airfoil with one experimentally specified degree of freedom in pitch are presented. The nonlinear system response for a variation of the Mach number and the mean angle of attack is investigated. Subcritical bifurcations and hystereses occur for both bifurcation parameters. The observed LCOs occur in the vicinity of the laminar drag bucket and are associated with significant changes in frequencies and phase differences between airfoil motion and aerodynamic forces. The results indicate a strong correlation between the shock-boundary layer interaction and the observed aeroelastic instability.

1 INTRODUCTION

Transonic flow over airfoils is inherently nonlinear [1], resulting from the presence of shocks, shock movement and shock-boundary layer interaction. Thus, even without any structural nonlinearity, the aeroelastic behavior of airfoils in transonic flow occurs as a nonlinear phenomenon, like limit cycle oscillations (LCOs) [2]. For laminar airfoils these aerodynamic nonlinearities are highly pronounced, as it has been shown for a CAST 10-2 supercritical laminar airfoil model in several studies [3–5]. The boundary layer of the airfoil is highly sensitive to disturbances in the vicinity of the characteristic drag bucket [6]. Small changes of the angle of attack lead to a distinct movement of the boundary layer, which interacts with the shock. Flutter experiments on the CAST 10-2 laminar airfoil have shown that the aeroelastic behavior is dominated by nonlinear effects as well. LCOs, among others, occurred within the transonic dip of the airfoil for a free transitional boundary layer. These were observed both for an aeroelastic configuration with two degrees of freedom (2-DOF), heave and pitch [7, 8], and for a configuration with one degree of freedom (1-DOF) in pitch [8]. In addition to the amplitude limitation, it was found that the aeroelastic 1-DOF configuration exhibits hysteresis and the LCO onset is described by a subcritical Hopf bifurcation rather than by a supercritical Hopf bifurcation [9]. The last flutter type is also called soft or ”good” flutter, whereas the subcritical case is described as hard or ”bad” flutter or LCO [10–12].

The aeroelastic system response for both bifurcation types is shown schematically in Fig. 1. If the system dynamics are described by a supercritical bifurcation (Fig. 1 left), the aeroelastic system moves on a stable path until the bifurcation point is reached, i.e. when the stability

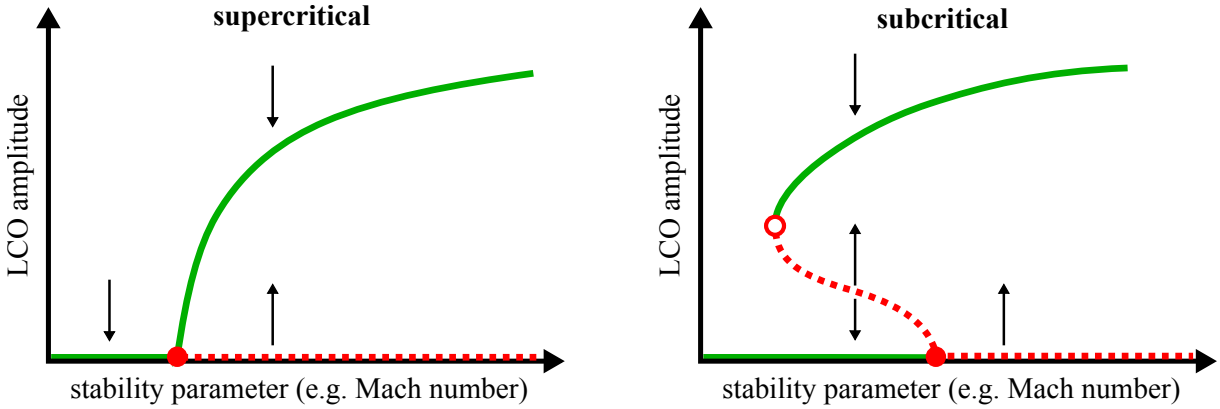

Figure 1: Schematic representation of the possible nonlinear aeroelastic system response, supercritical bifurcation (left) and subcritical bifurcation (right). The red dot marks the bifurcation point, i.e. the flutter speed in the classical sense. The red circle (right plot) marks the bifurcation point of a saddle-node bifurcation.

parameter (here the Mach number) is increased. When the bifurcation point is reached, the aeroelastic system begins to perform self-excited oscillations. The amplitude of these oscillations is limited (LCO) and increases with increasing Mach number. However, the system is still on a stable path or attractor. In case of a perturbation of the system, for example by an excitation, illustrated by arrows in Fig. 1, the system would return to this attractor. Furthermore, for this case the bifurcation point also corresponds to the critical flutter speed. As a result, the stability limit[1] of the aeroelastic system is clearly defined. If, however, there is a subcritical bifurcation (Fig. 1 right), this relationship is no longer unambiguous. When the bifurcation point is reached, the system also jumps to a stable limit cycle. However, a reduction of the stability parameter below the bifurcation point now does not lead to an immediate decay of the LCO. The system remains on this attractor until the Mach number is greatly reduced and the system returns to the initial stable path. On the other hand, it is also possible to move to the upper attractor just below the bifurcation point, so that the system undegoes LCOs in case of a perturbation. The necessary amplitude of the perturbation is illustrated in Fig. 1 right by the red dashed line. If the amplitude of the perturbation is below the repeller, the system remains on the first attractor and the perturbation is damped. However, if there is a perturbation with an amplitude above the repeller, it pushes the system into the basin of attraction of the upper attractor, thus a LCO occurs. So two stable states coexist for a certain range of the stability parameter between the bifurcation point of the saddle-node bifurcation (red circle in Fig. 1 right) and those of the subcritcal bifurcation (red dot in Fig. 1 right). Thus a bistability (coexistence of two stable states) or hysteresis exists. Two essential aspects for an aeroelastic system result from this. Firstly, the flutter point is now not unambiguously linked to the bifurcation point of the subcritical bifurcation. On the other hand, an aeroelastic instability can already occur below this bifurcation point within the bistability region if an excitation with sufficient amplitude is applied. This can occur, for instance, during strong turbulence, wakes or a gust [13, 14].

Aeroelastic systems with a hysteretic response or a subcritical bifurcation have been presented in several studies [10, 12, 15]. Often they were observed in connection with structural nonlinearities or stall flutter. In some cases, these also occur as secondary bifurcations [16, 17] which may also lead to nested LCOs [18] or several combinations of subcritical and saddle-node bifur-

[1] In this context, this refers to the point at which the system begins to carry out self-excited oscillations.

cations [19]. For transonic flow conditions results and observations of subcritical bifurcations of aeroelastic systems can be found in [2, 13, 14, 20]. First results of subcritical bifurcations or hystereses that occurred during the flutter test on the CAST 10-2 laminar airfoil are shown in [8, 9].

The paper presents results of the experimental bifurcation analysis, as it was performed for the aeroelastic 1-DOF configuration on the CAST 10-2 laminar airfoil. After a description of the experimental methodology for the measurement of subcritical bifurcations or hystereses, the bifurcation behavior for a variation of the Mach number and the mean angle of attack is discussed. Overall, the nonlinear response of the laminar airfoil or the aeroelastic system is analyzed more precisely. The paper provides a basis for further experimental and numerical investigations of the flutter stability of laminar airfoils and, in general, of aeroelastic systems in transonic flow, in which subcritical system responses have so far only been considered to a limited extent.

2 EXPERIMENTAL TEST SETUP

The present results were obtained by a 2D flutter experiment. The test was carried out in the Transonic Wind Tunnel Goettingen (DNW-TWG), which enables the Mach number to be fine-tuned by a thousandth with a measuring accuracy of Ma well below this small step size. The flutter test rig of the DLR Institute of Aeroelasticity [14] was used, which provides two experimentally specified degrees of freedom in heave and pitch. This 2-DOF configuration was reduced to a 1-DOF configuration in the process of the experiment as the heave DOF was mechanically locked. So, the laminar airfoil model was provided with one experimentally specified degree of freedom in pitch around the elastic axis ($e = c/4$). The whole flutter test rig was mounted into a 2D-support [14] in order to vary or adjust the mean angle of attack α_0 of the airfoil model. For the test a two dimensional CAST 10-2 supercritical laminar airfoil model was used, which was equipped with unsteady pressure sensors, accelerometers and hot-film sensors. The airfoil motion was measured by laser triangulators. Aerodynamic forces and moments were recorded by a spanwise integration of the pressure distributions. A more detailed description of the experimental setup is contained in [8], further notes can be found in [6, 9].

The measurements were performed in a Mach number range of $0.5 \leq \mathrm{Ma} \leq 0.8$ with a variable stagnation pressure p_0 of 40 kPa up to 75 kPa, hence the chord based Reynolds number Re_c varied between $1.15 \cdot 10^6$ to $2.83 \cdot 10^6$. All tests were performed with a free transitional boundary layer. For the investigation of the hysteretic response of the aeroelastic 1-DOF configuration, the Mach number and the mean angle of attack were varied. Since an experimental bifurcation analysis requires a special procedure, this is described in more detail in the following section.

3 MEASUREMENT PROCEDURE FOR BIFURCATION ANALYSIS

The investigation of hystereses or subcritical bifurcations of aeroelastic configurations requires a specific approach in the experiment. A common estimation of the stability limits of an aeroelastic system is generally done by successively increasing a stability or bifurcation parameter, usually the Mach number or the stagnation pressure. For the aeroelastic system considered here, LCOs first appear when the stability limit is exceeded, i.e. when entering the Transonic Dip of the CAST 10-2 laminar airfoil [8]. An increase of these stability parameters first leads to an increase of the LCO amplitude, until the considered LCOs become unstable and have to be stopped using a safety mechanism [6, 8, 21]. The bifurcation behavior obtained in this

way would therefore correspond to a supercritical bifurcation and the flutter limit would thus correspond to the bifurcation point, as shown in Fig. 1.

The flutter test rig of the DLR Institute of Aeroelasticity now enables a more detailed investigation of the nonlinear system response and a more precise resolution of the bifurcation behavior. For instance, the test rig is equipped with a flutter control system, which, in the case of an aeroelastic 2-DOF configuration, allows the excitation of the heave motion of the wind tunnel model [8, 13, 14]. This allows specified perturbations or an excitation with controllable amplitude to be applied below the stability limit. Using this flutter control system, in addition to measuring the stable branch of the bifurcation diagram, it is possible to resolve the unstable branch (repeller). Thus, for the CAST 10-2 laminar airfoil it could be shown that instabilities can also occur below the Transonc Dip, i.e. in the supposedly stable region, if a specific excitation amplitude is exceeded [8]. This shows that for the aeroelastic configuration with 2-DOF, the transition from the stable to the unstable region is (at least locally) described by a subcritical Hopf bifurcation. Consequently, a correspondence of the flutter boundary with the bifurcation point is not unambiguous, as already mentioned. In the case of the aeroelastic 1-DOF configuration examined here, the heave degree of freedom was locked (see section 2). The flutter control system only interacts with this degree of freedom and is therefore ineffective for the 1-DOF configuration. Consequently, a direct resolution of subcritical bifurcations, in particular the resolution of the repeller is not possible. Therefore, the system behavior was investigated indirectly by searching for hystereses in the vicinity of the stability limit, as described below.

For the consideration of the system behavior for a variation of the Mach number (see section 4.1) the Mach number was first increased incrementally until LCOs occurred. During the complete procedure the mean angle of attack was set to a constant value of $\alpha_0 \approx 0^\circ$. The Mach number was then further increased, whereby the entire aeroelastic system was not interrupted in any way. Just below the limit at which the observed limit cycle became unstable (limit known from previous measurement [8]), the Mach number was gradually reduced until the limit cycle oscillations disappeared. If the Mach number had been increased until an unstable limit cycle had occurred, it would have had to be stopped mechanically. This intervention would inevitably have massively disturbed the system behavior and would have been undesirable within the framework of a bifurcation analysis. For the observation of the system behavior under variation of the mean angle of attack (see section 4.2) α_0 was varied within a previously defined range using the 2D support mentioned in section 2. The mean angle of attack was first increased and then reduced again, whereby the Mach number was kept constant. In both cases, all other flow parameters were kept constant during the measurement in order to avoid any additional influence on the system behavior.

4 HYSTERETIC RESPONSE OF THE LAMINAR AIRFOIL

The nonlinear aeroelastic system behavior of the laminar airfoil is sensitive to a variety of parameters [9]. A control or specific regulation of these parameters in the experiment is not always completely possible in order to carry out a bifurcation analysis. The analysis of the nonlinear system behavior is therefore limited. In the present experimental context, well controllable stability parameters are the stagnation pressure p_0, the Mach number Ma and the mean angle of attack of the airfoil model α_0. A bifurcation analysis, as described in section 3, was performed as part of the flutter test for the latter two parameters. The results are discussed below.

4.1 Variation of the Mach number

For studying the influence of the variation in Mach number, the measurements were conducted at a constant stagnation pressure of $p_0 = 55$ kPa and a mean angle of attack of $\alpha_0 \approx 0°$ for a free transitional boundary layer. Although an aeroelastic 1-DOF configuration was provided, i.e. only a pitch DOF of the laminar airfoil model was experimentally specified, more recent investigations showed that during oscillations of the airfoil in pitch an additional bending of the airfoil model occurred as well [21]. The resulting heave motion of the airfoil's mid-section is relevant for an analysis of the aerodynamic power and is therefore also considered here.

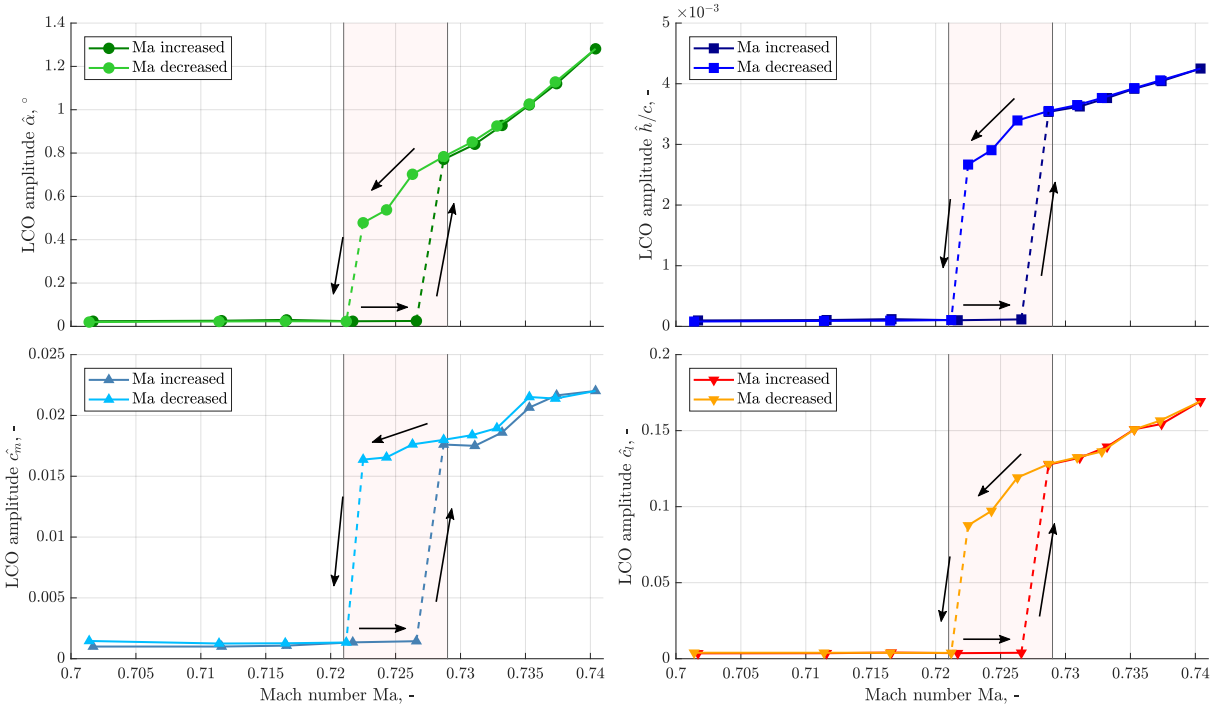

Figure 2: Bifurcation diagrams of the airfoil motion (top) as well as of the aerodynamic coefficients (bottom) for a variation of the mach number. The areas in which a hysteresis occurs are highlighted in red and additionally marked with arrows.

Fig. 2 shows the influence of the Mach number on the amplitude of the measured LCOs. In addition to the amplitudes of the aerodynamic coefficients $\hat{c}_l$ and $\hat{c_m}$ (bottom of Fig. 2), the LCO amplitudes of the motion of the mid-section of the laminar airfoil $\hat{\alpha}$ and $\hat{h}/c$ are plotted at the top of Fig. 2. The latter were calculated by filtering and integrating the signals of the local acceleration sensors twice. To calculate the LCO amplitudes, the envelopes of the LCOs were determined. For this purpose, a sliding averaging of 50 previously detected maxima and minima of the oscillations was performed. As can be seen in Fig. 2, an increase of the Mach number to $\mathrm{Ma} = 0.729$ leads to the occurrence of a first LCO. Thus a bifurcation point or the critical Mach number has been passed. A further increase leads to a growing LCO amplitude until a Mach number of $\mathrm{Ma} = 0.74$ is reached. For Mach numbers beyond $\mathrm{Ma} = 0.74$, where no measurement was performed in the present test case, the limit cycle becomes unstable [8]. Instead, the Mach number was reduced. The LCO amplitude decreases again and follows an almost identical trend as before. For a further reduction of the Mach number below $\mathrm{Ma} = 0.729$, the LCO continues to exists until $\mathrm{Ma} = 0.721$. So, a hysteretic response of the aeroelastic system occurs with a variation of the Mach number. The flutter onset is thereby described by a subcritical Hopf bifurcation. Consequently, this suggests the existence of an unstable

limit cycle between $0.721 \leq \mathrm{Ma} \leq 0.729$ which acts as a repeller. Unfortunately, a more precise resolution of the repeller is not possible in the experiment as mentioned in section 3. However, this suggests that a sufficiently large perturbation could push the system into the basin of attraction of the upper stable limit cycle. Thus the aeroelastic system could exhibit LCOs below $\mathrm{Ma} = 0.729$, even if the system comes from the lower attractor, i.e. from a state in which no oscillations are performed. The hysteresis indicates that, in contrast to a single critical value, a critical Mach number range of a width of approximately $\Delta\mathrm{Ma} \approx 0.01$ exists. This region is delimited by the bifurcation point of the subcritical bifurcation ($\mathrm{Ma} \approx 0.729$) as well as by the saddle-node bifurcation ($\mathrm{Ma} \approx 0.721$) and is highlighted in red in Fig. 2 and the following figures. It should also be noted that for all four LCO amplitudes considered, an approximately linear trend is present for a change of the Mach number as soon as the bifurcation point is exceeded. For the moment coefficient, these linear trend seems to be continued in the hysteresis region. For the pitch and especially for the heave and the lift coefficient, however, the amplitudes decrease slightly faster within a Mach number range of $0.723 \lesssim \mathrm{Ma} \lesssim 0.726$ than can be observed for higher Mach numbers.

Fig. 3 shows the development of the pitch frequency f_α during the variation of the Mach number. As can be seen in Fig. 3, the frequency rises significantly by about 6 Hz when the Mach number

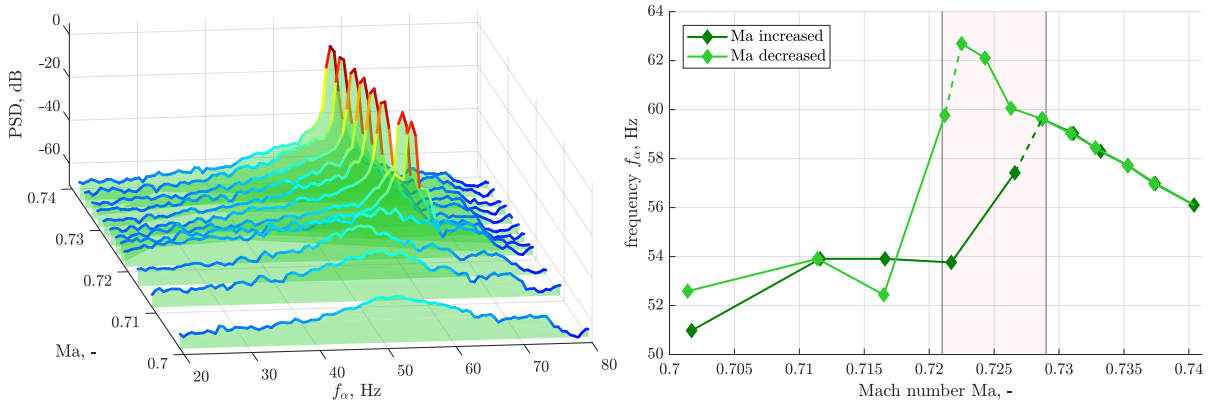

Figure 3: Power Spectral Densities (PSDs) of the pitch motion, displayed as a waterfall diagram (left) and detected frequencies $f_\alpha(\mathrm{Ma})$ during the bifurcation analysis. The hysteresis region is again highlighted in red.

is increased, before the first LCO occurs with a frequency of $f_\alpha \approx 60$ Hz. A further increase of Ma then corresponds to a decrease in frequency. During the reduction of the Mach number the frequency increases again and reaches frequencies above 62 Hz in the hysteresis range before an equally significant decrease of f_α occurs as soon as the aeroelastic system stops oscillating. So a hysteresis can also be clearly seen in the frequency trend. The characteristic frequency increase near the stability limit of the aeroelastic system has already been observed in [8]. In addition, an almost linear frequency trend can also be seen here, as already noted for the amplitude, although a slightly stronger increase in frequency is noticeable within the range $0.723 \lesssim \mathrm{Ma} \lesssim 0.726$.

A similar behavior can also be detected for the phase differences $\Delta\varphi_{x,y} = \varphi_x - \varphi_y$, which were evaluated at the respective frequencies mentioned above. The phase differences are shown in Fig. 4. The calculation was performed using an H1 estimator of the corresponding transfer functions. A hysteresis is also apparent in the trend of the phase differences. Especially for the phase difference between pitch and heave $\Delta\varphi_{\alpha,h}$ (Fig. 4 top left) as well as between pitch and the lift coefficient $\Delta\varphi_{\alpha,c_l}$ (Fig. 4 top right) the nearly linear trend is noticeable again as soon as the system is on the upper attractor. A reduction of the Mach number leads to the continuation

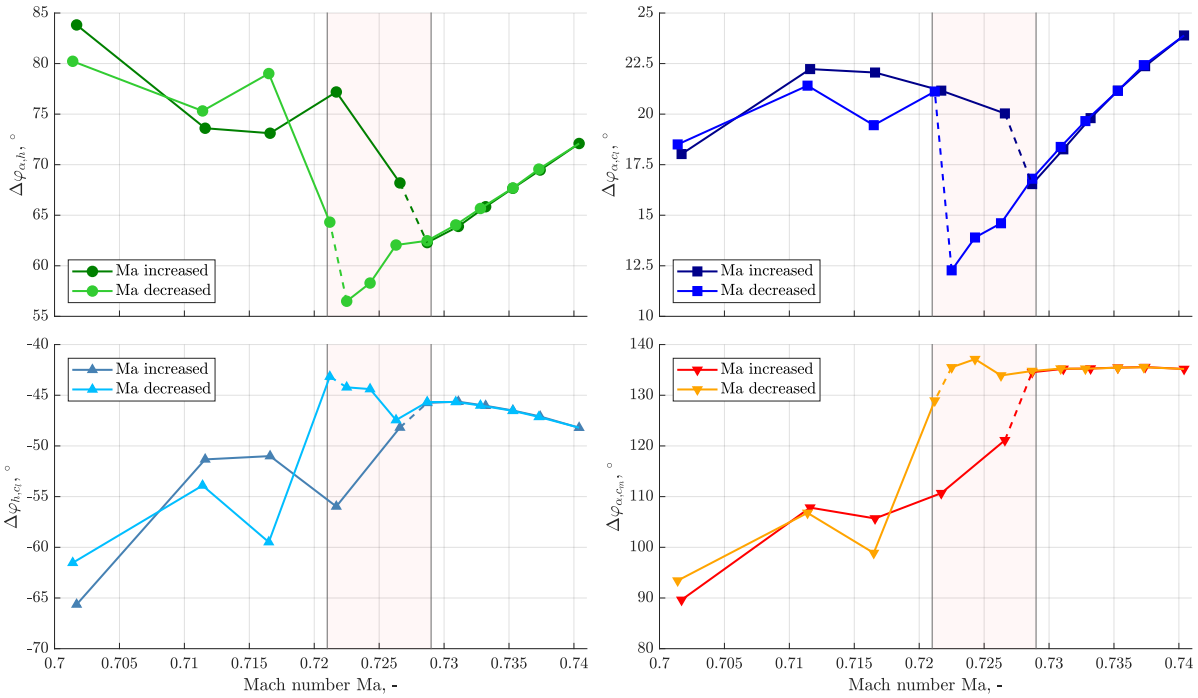

Figure 4: Phase differences between pitch and heave $\Delta\varphi_{\alpha,h}$ (top left), pitch and lift coefficient $\Delta\varphi_{\alpha,c_l}$ (top right), heave and lift coefficient $\Delta\varphi_{h,c_l}$ (bottom left) as well as pitch and pitching moment coefficient $\Delta\varphi_{\alpha,c_m}$ (bottom right), evaluated at the frequencies shown in Fig. 3.

of this linear trend in the hysteresis range. In both cases the phase difference decreases. In addition the phase differences between heave and lift coefficient $\Delta\varphi_{h,c_l}$ (Fig. 4 bottom left) and pitch and pitching moment coefficient $\Delta\varphi_{\alpha,c_m}$ (Fig. 4 bottom right) show a hysteresis and continue their trend when the Mach number is reduced. However, there are somewhat larger fluctuations around this trend. The absolute values of changes for $\Delta\varphi_{h,c_l}$ and $\Delta\varphi_{\alpha,c_m}$ are small. The phase differences remain nearly constant as long as the system is at the upper attractor. The mean value and the associated standard deviation of $-46.2° \pm 1.1°$ for $\Delta\varphi_{h,c_l}$ and $135.3° \pm 0.7°$ for $\Delta\varphi_{\alpha,c_m}$, calculated for the range where the system is located on the upper attractor, i.e. where it undergoes LCOs, confirm the constant trend, especially in the latter case.

The determined LCO amplitudes as well as the calculated phase differences were used to calculate the aerodynamic power averaged over one oscillation period. Under the assumption of a purely harmonic motion of the airfoil as well as of the aerodynamic forces and moments, the averaged aerodynamic power components can be written as

$$\bar{P}_l = -\frac{1}{2}\omega \frac{\hat{h}}{c} \hat{c}_l \cdot \sin(\varphi_h - \varphi_{c_l}) = -\frac{1}{2}\omega \frac{\hat{h}}{c} \hat{c}_l \cdot \sin(\Delta\varphi_{h,c_l}) \,, \tag{1}$$

$$\bar{P}_m = -\frac{1}{2}\omega \hat{\alpha} \hat{c_m} \cdot \sin(\varphi_\alpha - \varphi_{c_m}) = -\frac{1}{2}\omega \hat{\alpha} \hat{c_m} \cdot \sin(\Delta\varphi_{\alpha,c_m}) \,. \tag{2}$$

The average total aerodynamic power of one oscillation period then follows from the sum of the power of the lift $\bar{P}_l$ and the moment $\bar{P}_m$ according to $\bar{P}_{\text{ges}} = \bar{P}_l + \bar{P}_m$ [22]. The results for the Mach number variation are shown in Fig. 5. In accordance with the results in [21] it is shown that the lift feeds power or energy into the aeroelastic system (positive sign in Fig. 5 top left), whereas the aerodynamic moment damps the system (negative sign in Fig. 5 top right). A clear hysteresis is evident for both aerodynamic components as well as for the total aerodynamic power (Fig. 5 bottom). As expected, the total aerodynamic power averaged over one

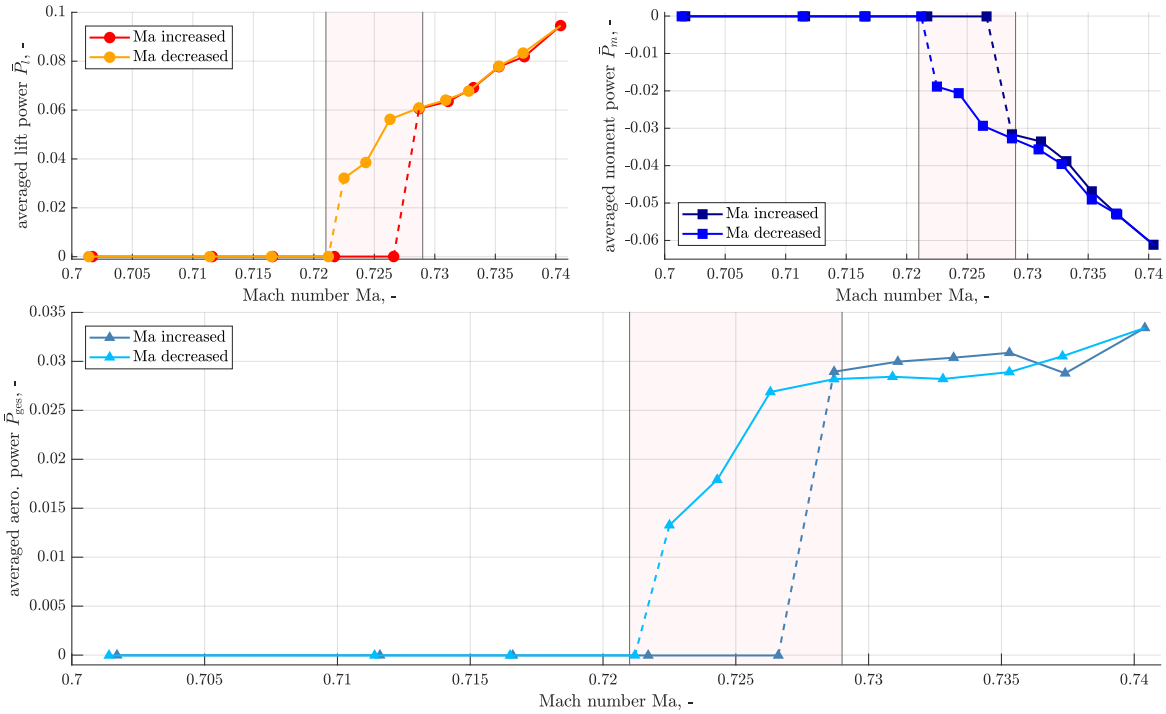

Figure 5: Aerodynamic power averaged over one oscillation period for a variation of the Mach number.

oscillation period increases with increasing Mach number, which correlates with the increase in LCO amplitude. The clearly recognizable decrease of the total power in the hysteresis range between $0.723 \lesssim \mathrm{Ma} \lesssim 0.726$ (Fig. 5 bottom) correlates with a decrease of the power of the lift in the same range (Fig. 5 top left). A closer look at Eq. (1) shows that this decrease is caused by the increased drop of the heave and lift amplitudes, as shown in Fig. 2 on the right. The phase difference $\Delta\varphi_{h,c_l}$ remains almost constant with variation of the Mach number, as already mentioned before, and therefore has a negligible influence.

Finally, the question arises why hystereses occur or why the response behavior of the aeroelastic system is described by a subcritical and not by a supercritical bifurcation. The behavior of the phase differences, shown in Fig. 4, may provide an indication for this. In particular, $\Delta\varphi_{h,c_l}$ and $\Delta\varphi_{\alpha,c_m}$ show nearly no change as long as the system is on the upper attractor. This indicates that the response behavior of the unsteady aerodynamics in the hysteresis range also remains unchanged. Thus, the underlying flow effects, in the present case in particular the unsteady shock-boundary layer interaction [21], also remain almost unchanged below the subcritical bifurcation point. However, the extent to which this is also the cause of the coexistence of two stable system states needs further investigation.

4.2 Variation of the mean angle of attack

In order to investigate the nonlinear system behavior for a variation of the mean angle of attack, α_0 was varied in the range $-1° \lesssim \alpha_0 \lesssim 0.7°$ for a constant Mach number of $\mathrm{Ma} = 0.73$ and a stagnation pressure of $p_0 = 55$ kPa. At Mach numbers above $\mathrm{Ma} = 0.73$, the observed LCOs became unstable several times, so that the aeroelastic system had to be stopped here [8]. For these cases the system behavior was disturbed. Thus, a bifurcation analysis was not performed for these conditions. The range in which α_0 was varied covers the region of the end of the characteristic laminar drag bucket of the CAST 10-2 laminar airfoil. This is depicted in Fig. 6, which shows the corresponding lift and pitching moment curve (left) as well as the airfoil's polar

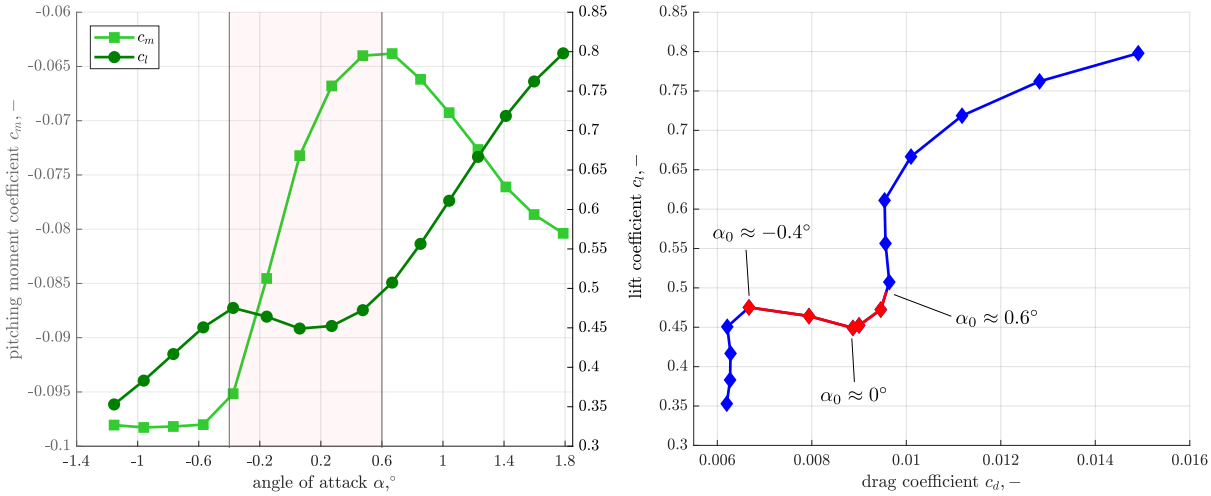

Figure 6: Lift and pitching moment curve (left) as well as polar of the laminar airfoil (right), measured at $\mathrm{Ma} = 0.73$ and $p_0 = 54$ kPa for a free transitional boundary layer, modified according to [9].

for $\mathrm{Ma} = 0.73$ (right). In a similar manner as was described in section 4.1, the LCO amplitudes were also calculated for a variation of α_0 and are displayed in Fig. 7. As can be seen, LCOs occur within a mean angle of attack range of $-0.4° \lesssim \alpha_0 \lesssim 0.6°$. This area is highlighted in red in the left part of Fig. 6 and marked by a red line in the polar. The occurring aeroelastic instability for $\mathrm{Ma} = 0.73$ correlates with the occurring plateau of the lift curve (Fig. 6 left) or the end of the laminar drag bucket (Fig. 6 right), as already described in [9]. In this area the position of the laminar-turbulent boundary layer transition is highly sensitive to a change in the angle of attack [6]. This suggests the strong connection between the occurrence of LCOs and the boundary layer transition, as discussed in [21].

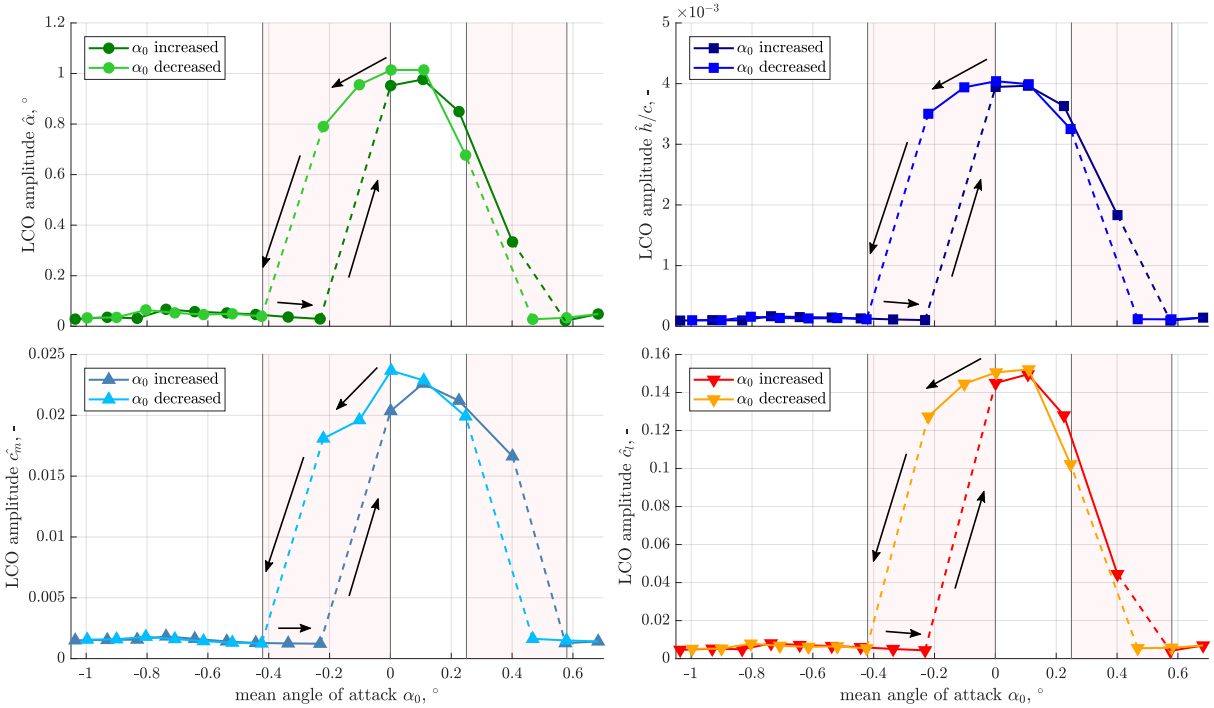

Figure 7: Bifurcation diagrams of the airfoil motion (top) as well as of the aerodynamic coefficients (bottom) for a variation of the mean angle of attack.

In addition to the connection of the aeroelastic instability to the laminar drag bucket, Fig. 7 also shows that subcritical Hopf bifurcations or hystereses also occur for a variation of the mean angle of attack. For this purpose α_0 was increased by an increment of $\Delta\alpha_0 \approx 0.1°$ using the 2D support (see section 2). It was found that LCOs occur for an increase of α_0 beyond a mean angle of attack of $\alpha_0 \approx 0.2°$. However, the amplitudes of the LCOs decreases very quickly upon a further increase in α_0. For a mean angle of attack of $\alpha_0 \approx 0.6°$ the LCOs completely vanish. A subsequent reduction of α_0 leads to self-excited oscillations occurring again at a slightly reduced mean angle of attack of $\alpha_0 \approx 0.45°$. A further reduction of α_0 initially leads to an increase of the LCO amplitudes, which follow approximately the previous trends. As soon as a mean angle of attack of $\alpha_0 \approx 0°$ is exceeded, the LCO amplitudes decrease again. For $\alpha_0 \lesssim -0.4°$ the system does not oscillate any more. Hence, a variation of the mean angle of attack results in two areas in which the nonlinear system response is characterized by a subcritical Hopf bifurcation, which are highlighted in red in Fig. 7. Especially the first hysteresis in the range $-0.4° \lesssim \alpha_0 \lesssim 0.0°$ is clearly visible. The hysteresis loop is additionally marked by arrows in Fig. 7. A second hysteresis occurs in the range $0.25° \lesssim \alpha_0 \lesssim 0.6°$, which becomes particularly clear in the trend of the amplitude of the aerodynamic moment coefficient $\hat{c}_m$ (bottom left of Fig. 7). However, the linear trends of the LCO amplitudes previously observed for a variation of the Mach number do not occur at all.

In addition to the hysteresis ranges, it can be seen that the system transition from one attractor to the other, i.e. the change between on- and offset of the LCOs, is combined with a jump in the mean angle of attack of approximately $0.1°$, as already shown in [9]. Although the mean angle of attack was varied by $\Delta\alpha_0 \approx 0.1°$, the aeroelastic system jumped by $\Delta\alpha_0 \approx 0.2°$ to its new mean angle of attack at the subcritical bifurcation points as well as at those of the saddle-node bifurcation. The hysteresis behavior is therefore combined with a weak divergence or a flutter divergent interaction and the bifurcation point seems to coincide with this additional effect [23]. So the system deliberately jumps from the lower to the upper attractor and vice versa, which makes a more detailed resolution of the hysteresis range much more difficult.

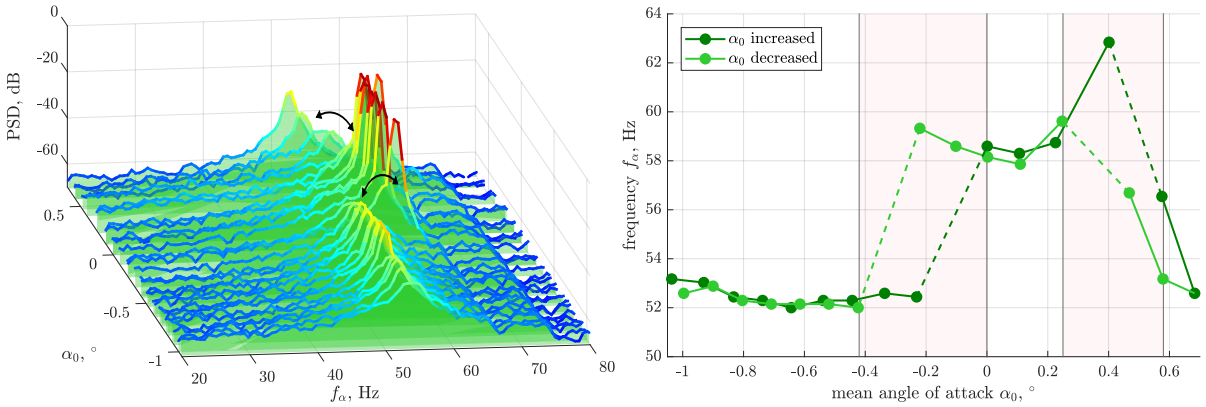

Figure 8: Change of the pitch frequency f_α with variation of the mean angle of attack. The corresponding PSDs are shown on the left as waterfall diagrams.

Overall, the observed flutter mechanism occurs in a limited range of angles of attack and forms a kind of ”island instability” for this bifurcation parameter. This also becomes evident when considering the frequencies of the LCOs or the aeroelastic system with a variation of the mean angle of attack, as shown in Fig. 8. An examination of the frequency development $f_\alpha(\alpha_0)$ shows, that as soon as the system moves to the upper attractor, this is combined with a significant increase in frequency. This is apparent in the area $-0.2° \lesssim \alpha_0 \lesssim 0.4°$ and is additionally

marked by arrows in the waterfall diagram (fig. 8 left). The characteristic increase in frequency just before LCOs occur for the aeroelastic 1-DOF configuration has already been observed for a variation of the Mach number (see section 4.1) and has been described in [8]. In Fig. 8, especially in the waterfall plot, it becomes even clearer that no continuous frequency transition occurs. Rather the frequency seems to jump from $f_\alpha \approx 52$ Hz to $f_\alpha \gtrsim 58$ Hz as soon as self-excited oscillations occur. Thereby, the "island-like" character of the instability is illustrated again.

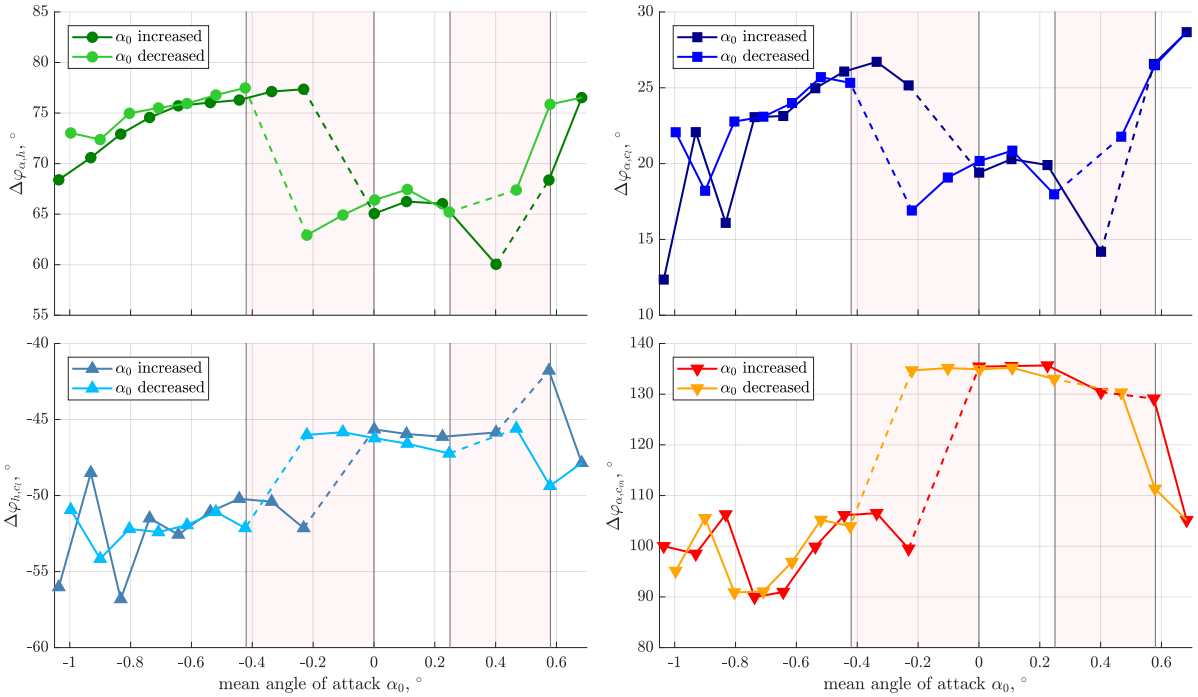

Figure 9: Phase differences for a variation of the mean angle of attack, evaluated at the frequencies shown in Fig. 8.

The hysteresis ranges become also obvious when considering the phase differences, depicted in Fig. 9. It can be seen, that there is a significant shift as soon as the system changes the attractor. The most obvious change occurs for the phase difference between the pitch and the moment coefficient in the first hysteresis range $-0.4° \lesssim \alpha_0 \lesssim 0.0°$. If the system changes the attractor, a jump of the phase difference of up to 35° occurs. The same applies to the second hysteresis range. A comparison with Fig. 6 shows that this correlates with the boundary regions of the laminar drag bucket or the regions in which the steady aerodynamic coefficients c_l and c_m also have a distinct nonlinearity. This significant change is closely linked to a variation of the shock-boundary layer interaction and thus confirms the significant influence of the boundary layer transition on the aeroelastic instabilities, as discussed in [21]. As already noted in section 4.1, the almost constant trends of $\Delta\varphi_{h,c_l}$ as well as $\Delta\varphi_{\alpha,c_m}$ where LCOs occur indicate that the unsteady aerodynamics remains largely unchanged. However, further investigations must also clarify the extent to which this is responsible for the occurrence of hystereses.

5 CONCLUDING REMARKS

With the accomplishment of experimental bifurcation investigations on the aeroelastic 1-DOF configuration of the laminar airfoil it was shown that the observed aeroelastic instabilities show hystereses. The nonlinear system response for a variation of the Mach number as well as for

a change of the mean angle of attack lead to a subcritical bifurcation behavior. This is evident not only from the evolution of the LCO amplitudes, but also from the change in frequencies and phase differences between the motion of the laminar airfoil and the aerodynamic forces. The strong correlation of the observed aeroelastic instability of the 1-DOF configuration with the end of the laminar drag bucket is particularly evident with a variation of the angle of attack. The sensitivity of the boundary layer transition to a change in the angle of attack confirms the considerable influence of the boundary layer transition in this region. This is further supported by the shift in frequency and in the phase difference between the pitch motion and the aerodynamic moment at the observed hysteresis ranges. However, the exact cause of the hystereses is the subject of further investigations.

Finally, it should be noted that the observed subcritical system transitions lead to stability limits, which cannot be determined with classical methods. It follows that both numerical and experimental methods must take these effects into account. For the analysis of aeroelastic systems, this requires a modified approach and the consideration of hystereses and subcritical bifurcations in order to ensure a largely complete and thus accurate estimation of stability limits. This should be achieved not only for laminar airfoils, but for any aeroelastic system with existing nonlinearities, e.g. for transonic flow conditions.

6 REFERENCES

[1] Bendiksen, O. (2011). Review of unsteady transonic aerodynamics: Theory and applications. *Progress in Aerospace Sciences*, 47(2), 135–167. doi:https://doi.org/10.1016/j.paerosci.2010.07.001.

[2] Schewe, G., Mai, H., and Dietz, G. (2003). Nonlinear effects in transonic flutter with emphasis on manifestations of limit cycle oscillations. *Journal of Fluids and Structures*, 18(1). doi:https://doi.org/10.1016/S0889-9746(03)00085-9.

[3] Hebler, A., Schojda, L., and Mai, H. (2013). Experimental investigation of the aeroelastic behaviour of a laminar airfoil in transonic flow. In *International Forum on Aeroelasticity and Structural Dynamics (IFASD), 24-26 June, Bristol, United Kingdom*.

[4] Fehrs, M. (2013). Influence of transitional flows at transonic mach numbers on the flutter speed of a laminar airfoil. In *International Forum on Aeroelasticity and Structural Dynamics (IFASD), 24-26 June, Bristol, United Kingdom*.

[5] Fehrs, M., van Rooij, A. C. L. M., and Nitzsche, J. (2015). Influence of boundary layer transition on the flutter behavior of a supercritical airfoil. *CEAS Aeronautical Journal*, 6(2), 291–303. doi: https://doi.org/10.1007/s13272-014-0147-7.

[6] Braune, M. and Koch, S. (2019). Application of hot-film anemometry to resolve the unsteady boundary layer transition of a laminar airfoil experiencing limit cycle oscillations. In *15th International Conference on Fluid Control, Measurements and Visualization (FLUCOME), May 27-30, Naples, Italy*.

[7] Hebler, A. (2017). Experimental assessment of the flutter stability of a laminar airfoil in transonic flow. In *International Forum on Aeroelasticity and Structural Dynamics (IFASD), 25-28 June, Como, Italy*.

[8] Braune, M. and Hebler, A. (2018). Experimental investigation of transonic flow effects on a laminar airfoil leading to limit cycle oscillations. In *Applied Aerodynamics Conference, AIAA AVIATION Forum, June 25-29, Atlanta, Georgia*. doi:https://doi.org/10.2514/6.2018-3641.

[9] Braune, M. and Hebler, A. (2019). Sensitivity of single degree of freedom limit cycle flutter of a laminar airfoil and resulting uncertainties of the transonic dip. In A. Dillmann, G. Heller, E. Krämer, C. Wagner, S. Jakirlic, and C. Tropea (Eds.), *New Results in Numerical and Experimental Fluid Mechanics XII*, Notes on Numerical Fluid Mechanics and Multidisciplinary Design. Springer. Accepted for publication.

[10] Dowell, E., Edwards, J., and Strganac, T. (2003). Nonlinear aeroelasticity. *Journal of Aircraft*, 40(5), 857–874. doi:https://doi.org/10.2514/2.6876.

[11] Bendiksen, O. O. (2004). Transonic limit cycle flutter/lco. In *45th AIAA/ASME/ASCE/AHS/ASC Structures, Structural Dynamics & Materials Conference, 19 - 22 April, Palm Springs, California*. doi:10.2514/6.2004-1694.

[12] Dowell, E. (2010). Some recent advances in nonlinear aeroelasticity: Fluid-structure interaction in the 21st century. In *51st AIAA/ASME/ASCE/AHS/ASC Structures, Structural Dynamics, and Materials Conference, Orlando, Florida*. doi:https://doi.org/10.2514/6.2010-3137.

[13] Dietz, G., Schewe, G., and Mai, H. (2004). Experiments on heave/pitch limit-cycle oscillations of a supercritical airfoil close to the transonic dip. *Journal of Fluids and Structures*, 19, 1-16. doi: https://doi.org/10.1016/j.jfluidstructs.2003.07.019.

[14] Dietz, G., Schewe, G., and Mai, H. (2006). Amplification and amplitude limitation of heave/pitch limit-cycle oscillations close to the transonic dip. *Journal of Fluids and Structures*, 22(4), 505–527. doi: https://doi.org/10.1016/j.jfluidstructs.2006.01.004.

[15] Lee, B., Price, S., and Wong, Y. (1999). Nonlinear aeroelastic analysis of airfoils: bifurcation and chaos. *Progress in Aerospace Sciences*, 35(3), 205–334. doi:https://doi.org/10.1016/S0376-0421(98)00015-3.

[16] Liu, L. and Dowell, E. H. (2004). The secondary bifurcation of an aeroelastic airfoil motion: Effect of high harmonics. *Nonlinear Dynamics*, 37(1), 31–49. doi:https://doi.org/10.1023/B:NODY.0000040033.85421.4d.

[17] Verstraelen, E., Kerschen, G., and Dimitriadis, G. (2016). Internal resonance and stall flutter interactions in a pitch-flap wing in the wind-tunnel. In G. Kerschen (Ed.), *Nonlinear Dynamics*, vol. 1 of *Conference Proceedings of the Society for Experimental Mechanics Series*. pp. 521–531. doi:https://doi.org/10.1007/978-3-319-15221-9_45.

[18] Bendiksen, O. (2017). Nested limit cycles in transonic flutter. In *International Forum on Aeroelasticity and Structural Dynamics (IFASD), 25-28 June, Como, Italy*.

[19] Eaton, A., Howcroft, C., Coetzee, E., et al. (2018). Numerical continuation of limit cycle oscillations and bifurcations in high-aspect-ratio wings. *Aerospace*, 5(3). doi:10.3390/aerospace5030078.

[20] Matsushita, H., Miyata, T., Christiansen, L., et al. (2002). On the nonlinear dynamics approach of modeling the bifurcation for transonic limit cycle flutter. In *23rd International Congress of Aeronautical Sciences, ICAS, 8-13 September, Toronto, Canada*.

[21] Braune, M. and Hebler, A. (2019). Mechanisms of transonic single degree of freedom flutter of a laminar airfoil. In *International Forum on Aeroelasticity and Structural Dynamics (IFASD), 9-13 June, Savannah, Georgia, USA*.

[22] van Rooij, A., Nitzsche, J., and Dwight, R. (2017). Energy budget analysis of aeroelastic limit-cycle oscillations. *Journal of Fluids and Structures*, 69, 174–186. doi:https://doi.org/10.1016/j.jfluidstructs.2016.11.016.

[23] Bendiksen, O. (1992). Role of shock dynamics in transonic flutter. In *Dynamics Specialists Conference, Dallas, TX, USA*. doi:https://doi.org/10.2514/6.1992-2121.

COPYRIGHT STATEMENT